Interaction of Al layers with polycrystalline Si †

K. Nakamura,* M-A. Nicolet, and J. W. Mayer

California Institute of Technology, Pasadena, California 91125

R. J. Blattner and C. A. Evans, Jr.

Materials Research Laboratory, University of Illinois, Urbana, Illinois 61801
(Received 13 May 1975)

Auger electron spectroscopy, MeV $^4He^+$ backscattering spectrometry and scanning electron microscopy have been used to investigate interactions between Al films and polycrystalline layers of CVD Si deposited on SiO_2. Depth profiling techniques showed that intermixing of the Al and Si occurred in the 400–560 °C temperature range (i.e., below the eutectic). Dissolution of the poly Si into the Al film occurs followed by nucleation and growth of Si crystallites in the Al film. The morphology of the final structure depends on the relative thicknesses of the as-deposited Al and Si layers. In the case of the original Al thickness being greater than that of the Si, the Si forms large precipitates in the Al matrix. For Al layers thinner than those of the Si, a nearly continuous Si film is formed on the outer surface. The thickness of this final Si film is approximately that of the original Al layer. The remaining Si and the Al form a two-phase layer between the outer Si film and the SiO_2 substrate.

PACS numbers: 68.50.

I. INTRODUCTION

Reactions between deposited Al films and single-crystal Si substrates have been widely studied because of their importance in integrated circuit fabrication.[1] During processing at temperatures below the Si-Al eutectic (577 °C), Si dissolves into the solid Al film. The solid solubility of Si in Al thin films is the same as that for bulk material.[1] The dissolution at the Si/Al interface occurs nonuniformly and forms pits which can penetrate shallow diffused regions. To overcome this problem, Si is usually codeposited with Al.[2] During heat treatment of these Al and Si films, Si present in excess of the solubility value at process temperature will form precipitates.[3,4]

Crystalline precipitates are also formed during heat treatment of amorphous Si in contact with metal films.[5] In the Si/Ag case, for example, the amorphous Si dissolves into the adjacent metal film. Subsequent diffusion and precipitation of the Si leads to growth of Si crystallites out of the solid metal solution.[6] During such isothermal treatments, all the amorphous Si can be transformed into crystallites. It is believed that the driving force for the growth is provided by the higher-energy state of the amorphous material compared with that of the crystalline material.[6] The solid metal layer provides the solvent and transport medium.

Polycrystalline silicon (poly Si) layers are used on dielectric layers in silicon gate MOS technology and on silicon for contact leads or diffusion sources. It has been reported[7] that a layer of poly Si between the aluminum metallization and Si single-crystal substrate can prevent the formation of dissolution pits on silicon devices during subsequent heat treatment.

In the present work, we have investigated the solid-phase reaction between poly Si and Al films in the temperature range 400—560 °C. Polycrystalline Si represents an intermediate structural form between single-crystal and amorphous Si. For poly Si produced by chemical vapor deposition (CVD) at temperatures of 650—750 °C, the grain size of undoped films grown on both silicon dioxide (as in the present case) and on bare silicon is of the order of 0.2 μm.[8]

Following heat treatment, the morphological changes in the poly Si/Al structure were monitored by scanning electron microscopy (SEM). Elemental depth profiles were obtained by MeV $^4He^+$ backscattering spectrometry (BS) and by Auger electron spectrometry (AES) combined with ion sputtering for sequential layer removal. These three techniques were combined to depict qualitatively the modifications which occurred during the solid-phase reactions between Al and Si.

II. EXPERIMENTAL PROCEDURES

A. Sample preparation

Polished single-crystal Si wafers of 4 ± 2-Ω cm n-type conductivity and oriented in ⟨100⟩ direction were thermally oxidized at 950 °C in steam to a thickness of 1000 ± 50 Å. The substrates thus obtained were covered with a layer of undoped polycrystalline Si formed at 640 °C by CVD. The polycrystalline nature of the deposited films was confirmed by electron diffraction analysis, but no direct measure of crystallite size was made. The thickness of this polycrystalline Si film ranged from approximately 0.3 to 0.5 μm. Finally, Al was vacuum deposited onto the polycrystalline Si by e-gun evaporation. The original thickness of this Al film was 1.2 μm in all cases. For experiments when thinner Al films were desired, the Al film thickness was reduced by chemically etching the wafer in an aqueous solution of 1N NaOH. To completely remove all Al for SEM observation, aqua regia was used. Anneals were performed in either dry N_2 or in vacuum. No difference was observed in the results obtained with either of the two ambients. All anneals were performed below the 577 °C eutectic temperature of Al-Si.

B. Backscattering spectrometry

The experimental setup and analytical method for backscattering spectrometry have been reviewed elsewhere.[9] In brief, the technique consists of placing a

sample in a beam of monoenergetic helium ions and energy analyzing the particles scattered back and out of the sample. Backscattering spectrometry with MeV $^4He^+$ ions provides information on elemental concentration profiles with a depth resolution of about 200 Å for layers as thick as 5000 Å. With thicker films the depth resolution degrades due to the energy straggling of the probing particle. The beam spot is typically 1—2 mm^2. Hence, backscattering averages the composition of a sample over lateral dimensions of this magnitude.

C. Auger electron spectrometry

A Physical Electronics model 545 scanning Auger microprobe was used for all Auger electron spectroscopic measurements.[10,11] The samples were mounted on the standard carrousel at 30° grazing incidence for the primary electron beam. The residual vacuum of the sample chamber was $<1\times10^{-9}$ Torr prior to all analyses. Primary electron energies of 6 keV were employed. Elemental depth profiles were made by monitoring the Si, Al, and oxygen Auger transitions with simultaneous 2-keV Ar^+ ion sputtering for removal of successive atomic layers.

D. Scanning electron microscopy

Scanning electron micrographs were taken on an Akashi-Seisakusho model MSM-2 Mini-SEM and on a JEOLCO model U3.

III. RESULTS AND DISCUSSIONS

The main result of this work is that polycrystalline Si in contact with an aluminum film dissolves, migrates, nucleates, and forms crystalline precipitates in the Al matrix. The rates are such as to lead to major modifications in the Si structure for annealing times as short as 15 min at 400 °C. The morphology of the Si/Al bilayer after annealing depends on which of the two films (poly Si or Al) is originally the thicker one.

A. Al layer thicker than the poly Si layer

1. SEM micrographs

Samples of 0.5-μm-thick poly Si covered with approximately 1 μm of Al were annealed for 30 min between 400 and 500 °C. Figure 1(a) shows an SEM micrograph of a poly Si surface which was not subjected to any annealing. Figures 1(b) and 1(c) are micrographs of the samples annealed at 400 and 440 °C. In all cases, the Al was chemically removed before examination. As can be clearly seen, the anneal treatment induces the growth of micrometer-size precipitates. These are not dissolved by the etch and must therefore be Si. This identification is further supported by the BS and AES measurements discussed below. A crystallographic study of the individual precipitates seen in these micrographs has not yet been made, but the faceted shapes suggest high crystalline order within each precipitate. Their identification as Si crystallites has been confirmed independently by x-ray diffraction pictures taken on a Read camera.[12] After anneal, Debye-Scherrer rings appear which consist of a multitude of individual spots. The rings are absent before the anneal.

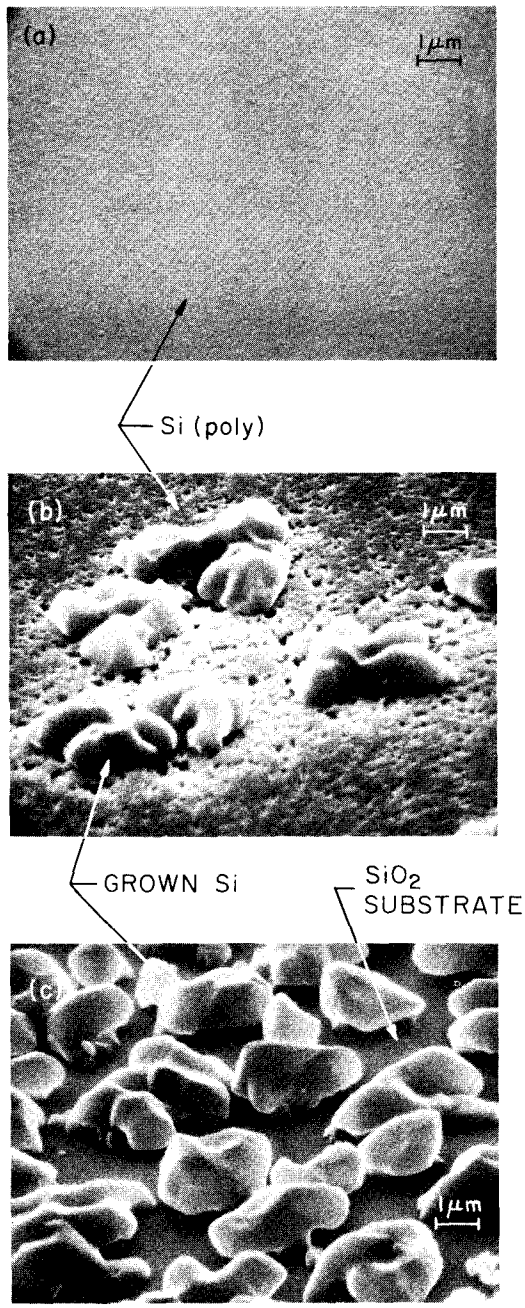

FIG. 1. Scanning electron micrographs of samples with 1 μm Al on 0.5-μm poly Si (a) before annealing and after annealing for 30 min at (b) 400 °C and (c) 440 °C. The Al was chemically removed before examination in all cases. The incident angle of the electron beam with respect to the normal of the sample is 60°.

In Fig. 1(b), the substrate on which the crystallites rest shows voids and pits indicative of the erosive effect of the Al film [compare with Fig. 1(a)]. BS positively identifies the material of this substrate as poly Si. Contrasting with Fig. 1(b), the substrate in Fig. 1(c) is smooth, and the crystallites are larger and more numerous. This micrograph depicts a state when all of the original polycrystalline Si layer has been converted to Si crystallites. The substrate exposed after the Al etch is thus SiO_2. This was verified by a back-

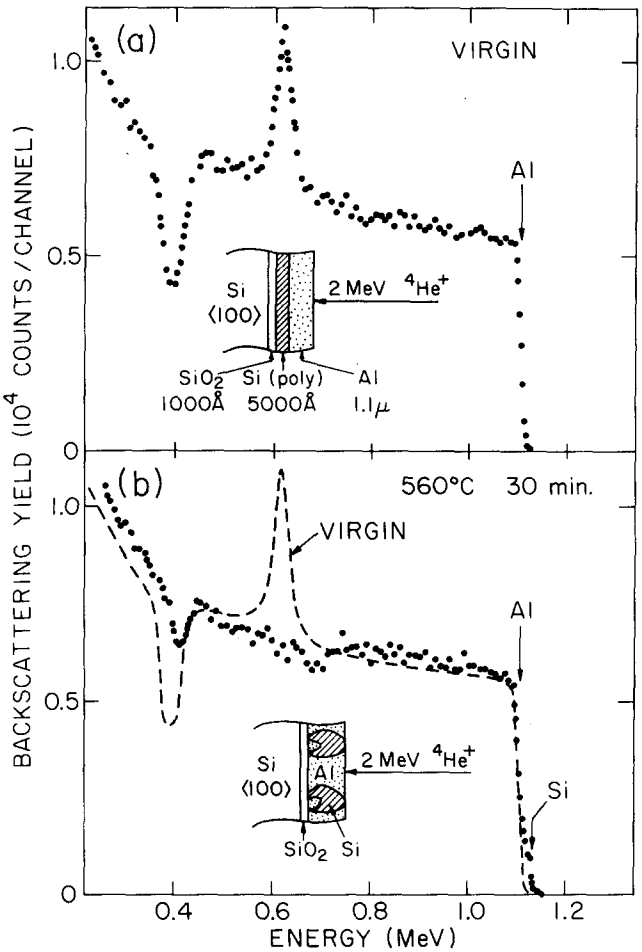

FIG. 2. Backscattering spectra of samples with 1.1 μm Al on 0.5 μm poly Si (a) before annealing and (b) after annealing at 560 °C for 30 min. The arrows indicate the energy corresponding to scattering from atoms at the surface.

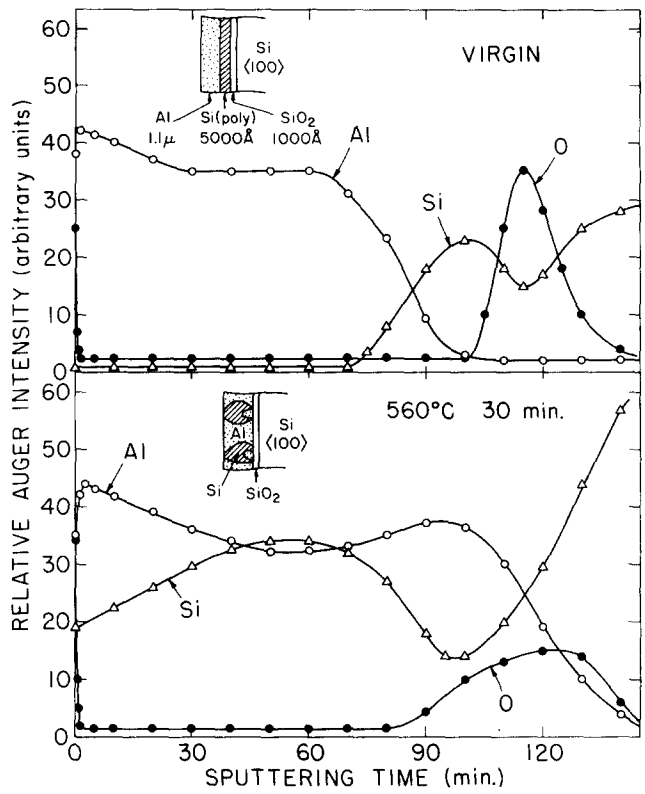

FIG. 3. Auger depth profiles of Al, Si, and oxygen of the samples with 1.1 μm Al on 0.5 μm poly Si (a) before annealing and (b) after annealing at 560 °C for 30 min. Intensity units are adjusted for clarity of display for each element.

scattering analysis of the sample shown in Fig. 2(c). The oxygen signal was found to extend all the way to the surface. An independent confirmation that all the poly Si is transported is provided by the fact that an anneal treatment of the same duration at a higher temperature (490 °C) leads to a similar morphology.

Two observations are of further interest. The size of the crystallites varies, but their height is confined to the thickness of the original Al layer thickness (~1 μm) or less. This is also the conclusion one draws from micrographs of the surface of samples annealed to the final state but from which the Al has not yet been removed. Their surface is fairly smooth with a very few of the crystallites detectable as protrusions above the Al layer. Second, a careful inspection of micrographs such as that of Fig. 1(c) reveals that most of the crystallites do not make contact with the SiO_2 substrate over their full cross section.

2. AES and BS analysis

Fully reacted samples annealed at 560 °C for 30 min have also been analyzed by BS and AES. Figures 2(a) and 2(b) show backscattering spectra before and after annealing, and Figs. 3(a) and 3(b) show the corresponding Auger depth profiles of Al, Si, and oxygen for samples of identical origin and treatment. In the backscattering spectrum of the virgin sample [Fig. 2(a)], the dip in the spectrum at 0.4 MeV indicates the SiO_2 layer and the peak at 0.6 MeV marks the interface between the poly Si and the Al.[13] Both features in this spectrum are very well resolved indicating sharp interfaces between the various layers in the multilayer structure. Note, however, that the corresponding Auger depth profiles of Fig. 3(a) display much smoother transitions at the interfaces for all three elements. This apparent inconsistency between the results of BS and AES is caused by local variations of the sputtering rates in the polycrystalline Al. The disagreement is thus not real but an artifact caused by the sputtering process.

After sample annealing, the backscattering spectrum changes quite noticeably [see Fig. 2(b)]. The lateral nonuniformity of the sample as revealed in Fig. 1(c) makes it difficult to interpret the backscattering spectrum, however. The spectrum of Fig. 2(b) nevertheless contains two useful pieces of information which hold in spite of the lateral nonuniformity: (i) the high-energy edge of the spectrum contains a small but significant step which coincides with the backscattering signal of Si atoms at the surface of the sample; (ii) there is a small but definite dip in the spectrum at approximately 0.7 MeV. The first observation establishes that during the anneal Si atoms have migrated from the underlying polycrystalline layer to the surface of the sample. This confirms the earlier identification of the crystallites as being silicon. The second feature of the spectrum can only be explained by the existence of an interface

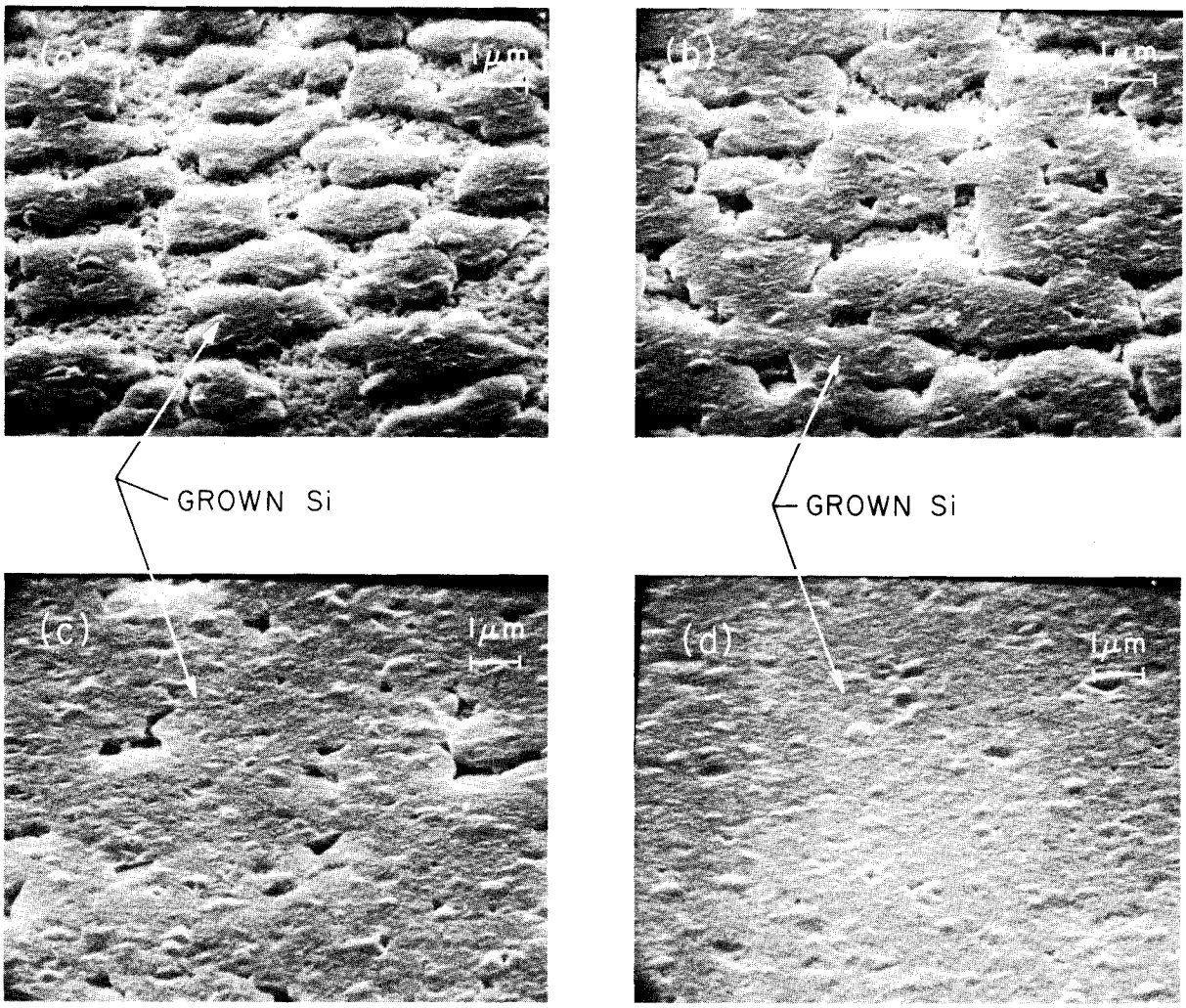

FIG. 4. Scanning electron micrographs of samples with 0.25 μm Al on 0.35 μm poly Si after annealing at 400°C for (a) 15 min, (b) 30 min, (c) 1 h, and (d) 2 h. The Al was chemically removed before examination. The incident angle of the electron beam with respect to the normal of the sample is 60°.

between Si overlying Al at a depth corresponding very roughly to the thickness of the original Al film. We attribute this interface to the presence of Al under the Si crystallites where they do not contact the SiO_2 substrate (see inset). The dip in the spectrum at 0.7 MeV is ill defined because the shape and size of the Si voids varies from one crystallite to another.

The Auger spectra of Fig. 3(b) are more difficult yet to interpret than Fig. 3(a) because the different sputtering rates of the Si crystallites and the Al matrix produce a nonuniform sputtering front. This uneven surface causes a distortion of the AES depth profiles. Useful information is nevertheless provided by these spectra. The presence of Si and Al at the surface (at time zero) confirms that the Si crystallites do extend throughout the Al layer. The apparent persistance of the Al and Si signals into the region of the SiO_2 confirms the BS and SEM results that Si and Al are present throughout the layer above the SiO_2.

B. Al layer thinner than the poly Si layer

The results obtained for the thick Al layer described above demonstrate that Al acts as a transport and growth medium for Si. To gain further insight, films were annealed and characterized in which a thickness constraint was placed on the Al medium. One such set of samples consisted of films with 0.25 μm of Al on 0.35 μm of poly Si on SiO_2 which were annealed at 400 °C for 15, 30, 60, and 120 min. The resultant samples were etched in aqua regia to remove the Al, as was done for the thick Al samples, and then examined by SEM. The micrographs of these etched samples are shown in Figs. 4(a)–4(d). Figure 4(a) shows islands of transported and precipitated Si above the partially consumed and eroded poly Si. Figures 4(b), 4(c), and 4(d) show that this process of dissolution, transport, and precipitation progresses with time until the Si crystallites coalesce into an essentially continuous layer. The displacement of the Al medium to the region originally occupied by the Si is revealed by the AES and BS analyses of Figs. 5 and 6 which refer to samples annealed at 560° for 30 min.

The AES depth profile of Fig. 5 shows that the outer layer is essentially pure Si over an inner layer containing some Si and most of the displaced Al. Two features in this profile lead one to believe that this Al-rich inner

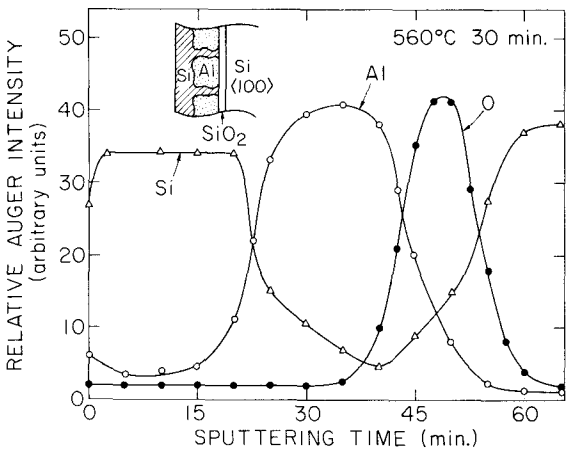

FIG. 5. Auger depth profiles of Al, Si, and oxygen of a sample with 0.3 μm Al on 0.35 μm poly Si after annealing at 560 °C for 30 min. Intensity units are adjusted for clarity of display for each element.

layer is a multiphase region. The concentrations indicated by the relative Al and Si Auger intensities in the 25—40 min region is much greater than the solubility of Si in Al expected from the phase diagram.[14] Second, the lack of sharpness of the Al/SiO_2 interface in this depth profile strongly suggests lateral inhomogeneities and consequently an irregular sputtering front during the AES depth profile. The BS spectrum of Fig. 6 confirms the existence of an outer Si-rich layer in the annealed film but provides no insight on the multiphase nature of the underlying Al/Si region. To examine the inner Al-rich layer by chemical etching and SEM observation, the outer Si-rich layer was removed by ion sputtering. This was accomplished by monitoring the Al Auger transition while ion etching with 2-keV Ar^+. After sputtering away the Si-rich layer and exposing the Al-rich layer, the sample was chemically etched to remove the Al. The resultant micrograph of Fig. 7 shows that this layer contains Si crystallites in a matrix of the displaced Al.

Figure 6(b) also reveals that the thickness of the outer Si layer in the final state is approximately equal to that of the initially deposited Al. To investigate this point, a series of samples was prepared with a factor-of-4 variation in the Al layer thickness. The poly Si layer was approximately 5000 Å thick in all cases. BS was then used to quantitatively determine the thickness of the Al in the virgin samples and the thickness of the top Si layers in the final state. The results are shown in Fig. 8. These data establish clearly that the original Al thickness prescribes the final Si thickness when there is less Al than Si.

IV. CONCLUSIONS

A. Morphology

The main conclusion of this study is that poly Si which is in contact with a film of solid Al will be dissolved and transported in the Al, and it will then precipitate in crystalline form out of the Al at temperatures well below that of the eutectic. Simultaneously, the Al is displaced by the growing Si crystallites. The morpholo-

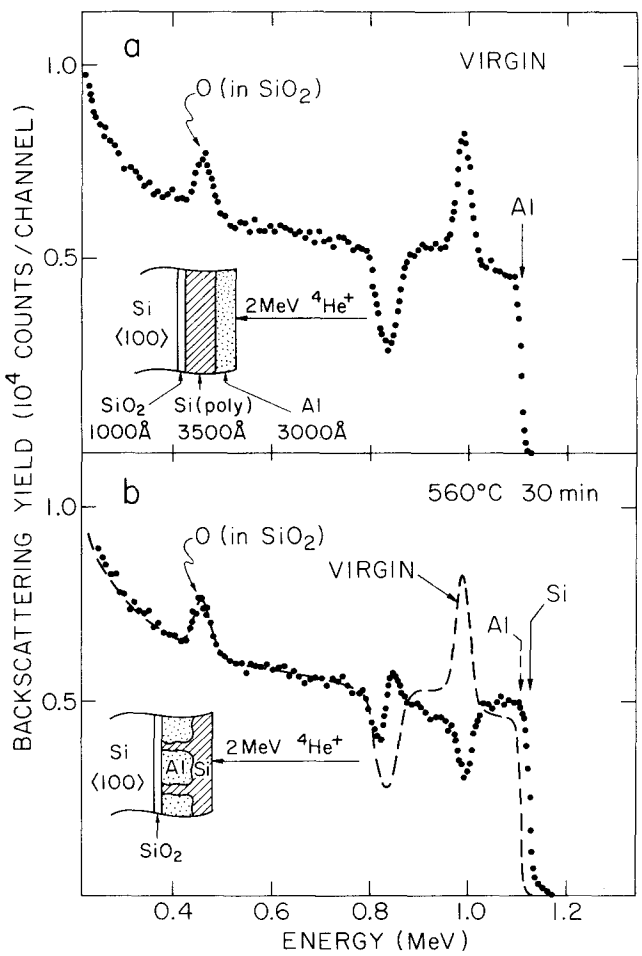

FIG. 6. Backscattering spectra of samples with 0.3 μm Al on 0.35 μm poly Si (a) before annealing and (b) after annealing at 560 °C for 30 min.

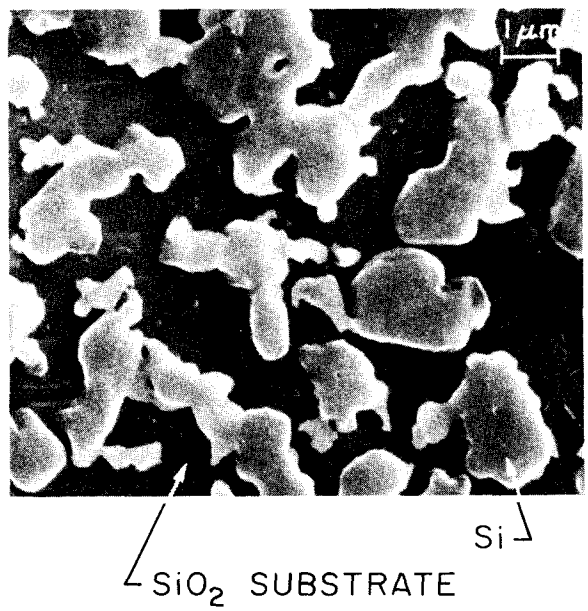

FIG. 7. Scanning electron micrograph of the sample in Fig. 5 after sputtering away the outer Si-rich layer and chemically removing the residual Al.

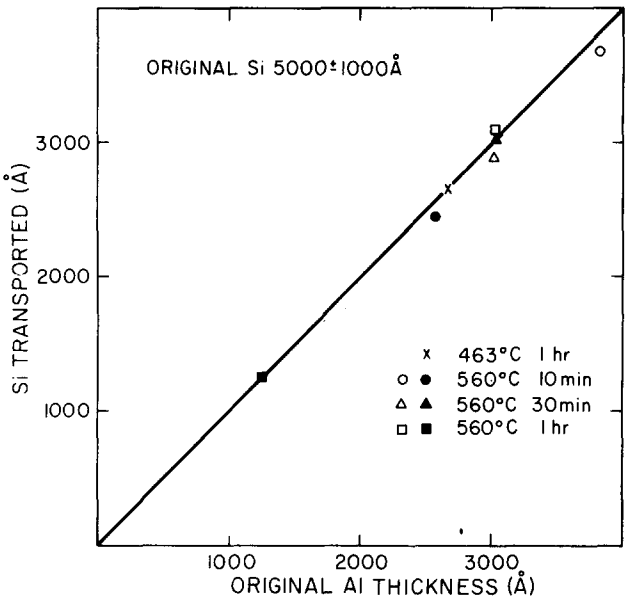

FIG. 8. Thickness of the Si layer transported to the surface as a function of the original Al thickness determined from backscattering spectra such as those shown in Fig. 6(b).

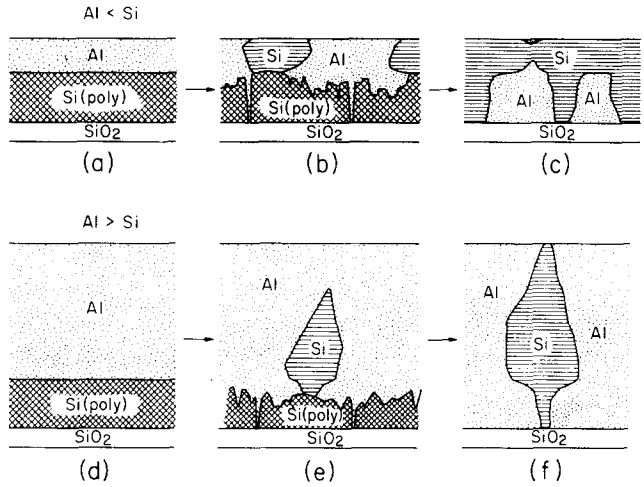

FIG. 9. Schematic diagrams showing the changes which occur during annealing for samples with original Al layer thinner than the poly Si layer [(a), (b), and (c)] and for samples with original Al layer thicker than the poly Si layer [(d), (e), and (f)].

gy of these Si crystallites is controlled by the amount of Al present. If the Al film is initially thinner than the polycrystalline Si, the precipitating Si is constrained to grow in the lateral direction once the crystallites have reached the dimension of the Al film thickness. The lateral growth comes to an end when the Al film has been displaced by an almost continuous layer of Si crystallites of roughly the same thickness as the original Al film. The remaining poly Si precipitates in the space first occupied by the Si and forms pillerlike connections between the top Si layer and the SiO_2 substrate. The voids around these Si pillars are filled by the displaced Al.

When the Al film is initially thicker than the poly Si, the growth of the Si crystallites will come to an end before a continuous Si layer is formed. In this case, Si precipitates in the form of distinct crystallites. The Al is again displaced into the area first occupied by the now dissolved Si. The space between the base of the crystallites and the SiO_2 substrate again contains pillarlike bridges of Si connecting the crystallites and the substrate.

A schematic representation of the changes which take place during anneal is given in Fig. 9. The sketches are correct only in their gross features, because most of the details have yet to be elucidated. As the sketches reveal, the difference in the final shape of the recrystallized Si obtained with thin or with thick Al layers reflects the difference in external constraint exerted on the system during anneal. On the microscopic scale, the two cases appear to be indistinguishable.

B. Speculations

It is natural to inquire of the deeper causes for the effects described above. Morphological observations of the kind presented here do not expose the developments at the atomic scale; they are expressions of them. An interpretation of the observations at this deeper level is therefore speculative. We present here some views on possible reasons. Future experiments—perhaps inspired by these speculations—will have to substantiate or refute these ideas.

We propose that poly Si recrystallizes because the resultant crystallites are substantially larger in size than those originally present in the polycrystalline layer. The silicon thus moves from a state of higher to one of lower total energy. This hypothesis is consistent with other known facts. Amorphous films of Si in contact with appropriate transport media also recrystallize at similarly low temperatures.[6] Amorphous Si layers on single-crystal Si obtained by ion implantation have been seen to recrystallize at equally low temperatures (450–500 °C) although there is no transport medium to assist the process there.[15] On the other hand, Al films deposited on wafers of single-crystal Si only induce a (reversible) dissolution of Si in the Al.[3] Similar results hold for Al films on Ge single crystals.[16] This last example underlines that the hypothesis indeed makes no reference to a specific substance. The effects observed here for Si should thus be common to amorphous or polycrystalline layers of many materials.

Assuming that the hypothesis is correct, the question then arises as to how small the grains in the polycrystalline layer must be to promote the effect of recrystallization. The answer must depend on the thickness of the transporting layer (Al in our case), because this thickness limits the size of the crystallites in the dimension perpendicular to the substrate. All other parameters remaining constant, recrystallization is conceivable if the thickness of the transporting layer is large compared to the grain size of the polycrystalline layer. Otherwise, recrystallization will not occur, as is indeed the case for single-crystal substrates.

In addition to these geometrical factors, metallurgical effects must influence the recrystallization process as well. It is more difficult to speculate on the role which the transport layer plays here. How significant

are the effects of grain size, grain boundaries, mutual solubilities, ductility, stress, impurities, and defects in this "transport" layer? One can readily see that any one of these characteristics could suppress the recrystallization process by modifying them appropriately. It will require substantially more information on a number of systems to clarify these issues. The problem is probably complex considering the number of relevant parameters.

C. Analytical considerations

The main analytical techniques employed in this study are (i) SEM, (ii) AES, and (iii) BS. This particular choice—which was obtained by effective cooperation of individuals in two separate institutions—is the result of a conscientious effort to combine a few modern analytical tools in such a way that each method provides accurate information where the others fail. We believe that SEM, AES, and BS form such a well-balanced set of tools for the study of crystallization processes on solid surfaces and in thin films.

SEM has the microscopic lateral resolution which is essential for the visualization of the modifications which take place on the surface and which is also a safeguard against erroneous interpretations of Auger and backscattering spectra. Both Auger and backscattering data must be interpreted with extreme caution when applied to laterally nonuniform samples. The difficulties in interpreting profiles have been shown directly in the present work and in other studies of nonuniform samples.[6,17] An SEM micrograph, however, gives only geometrical contours with no chemical identification. The latter is provided with high specificity by AES, but this method is slow and the information is obtained only on relative scales of intensity and depth. By contrast, BS is fast and yields absolute values for the depth and the atomic ratios of elements present. Frequently, however, the atomic specificity of BS is woefully inadequate, and the poor sensitivity to low atomic masses constitutes a severe handicap.

Except for the use of selective removal by chemical etching and a few x-ray diffraction photos, the processes sketched in Fig. 9 have been clarified and characterized entirely by judicious use of SEM, AES, and BS. Any one of these techniques alone would have been unable to accomplish this. The success of this study supports our contention that SEM, AES, and BS together constitute an analytical capability of much power. This investigation may thus also stand as a helpful model for further studies of a similar kind.

ACKNOWLEDGMENTS

The authors thank Sylvanus S. Lau for his assistance with the x-ray diffraction pictures taken on a Read camera, and for his constructive participation throughout the investigation. They also acknowledge the help of Mototaka Kamoshida, Nippon Electric Co., Ltd., Kawasaki, Japan, who provided poly Si samples.

†Work supported in part by National Science Foundation Grants MPS 74-05745 and DMR 72-03026 at the University of Illinois and in part by grants of the Ford Foundation (T. Cole) and the Gulf Oil Foundation (A. Lewis, Jr.) at the California Institute of Technology.

*Permanent address: Nippon Electric Company, Ltd., Kawasaki, Japan.

[1]J. O. McCaldin and H. Sankur, Appl. Phys. Lett. **19**, 524 (1971).
[2]P. A. Totta and R. P. Sopher, IBM J. Res. Dev. **13**, 226 (1969).
[3]J. O. McCaldin and H. Sankur, Appl. Phys. Lett. **20**, 171 (1972).
[4]G. J. van Gurp, J. Appl. Phys. **44**, 2040 (1973).
[5]S. R. Herd, P. Chaudhari, and M. H. Brodsky, J. Non-Cryst. Solids **7**, 309 (1972).
[6]G. Ottaviani, D. Sigurd, V. Marrello, J. W. Mayer, and J. O. McCaldin, J. Appl. Phys. **45**, 1730 (1974).
[7]S. P. Bellier and L. B. Ehlert, in *Semiconductor Silicon* 1973, edited by H. R. Huff and R. R. Burgess (The Electrochemical Society, Princeton, N. J., 1973), p. 304.
[8]P. Rai-Choudhury and P. L. Hower, J. Electrochem. Soc. **120**, 1761 (1973).
[9]W. K. Chu, J. W. Mayer, M-A. Nicolet, T. M. Buck, G. Amsel, and F. Eisen, Thin Solid Films **17**, 1 (1973).
[10]C. C. Chang, in *Characterization of Solid Surfaces*, edited by P. F. Kane and G. R. Larrabee (Plenum, New York, 1974).
[11]J. M. Morabito, Thin Solid Films **19**, 21 (1973).
[12]M. H. Read and D. H. Hansler, Thin Solid Films **10**, 123 (1970); see also S. S. Lau, W. K. Chu, J. W. Mayer, and K. N. Tu, Thin Solid Films **23**, 205 (1974).
[13]I. V. Mitchell, M. Kamoshida, and J. W. Mayer, J. Appl. Phys. **42**, 4378 (1971).
[14]M. Hansen, *Constitution of Binary Alloys* (McGraw-Hill, New York, 1958).
[15]L. Czepregi (private communication).
[16]J. M. Caywood, Metall. Trans. **4**, 735 (1973).
[17]S. U. Campisano, G. Foti, F. Grasso, and E. Rimini, Thin Solid Films **25**, 431 (1975).